ELSEVIER

Thin Solid Films 361–362 (2000) 243–247

thin solid films

www.elsevier.com/locate/tsf

Electron-paramagnetic resonance (EPR) and light-induced EPR investigations of $CuGaSe_2$

M. Birkholz*, P. Kanschat, T. Weiss, K. Lips

Hahn-Meitner-Institut, Abteilungen AP & FH, Kekuléstraße 5, D-12489, Berlin, Germany

Abstract

The chalcopyrite compound $CuGaSe_2$ is considered as potential absorber material for thin film solar cells due to its suitable optoelectronic properties. We investigated intentionally undoped bulk material that is used as source material in a thin film deposition process by electron-paramagnetic resonance (EPR) and light-induced EPR (LEPR). Both methods are well suited to determine the concentration and electronic activity of transition metal ions in the chalcopyrite host lattice. The recently identified Ni^+ centre was found by LEPR to act as recombination centre for photogenerated charge carriers. Moreover, the typical signature of Cu^{2+} could be detected in EPR spectra of aged $CuGaSe_2$ powders indicating an oxidation process to which the material is subjected at ambient conditions. The ageing process is significantly accelerated in water-saturated air of 100% humidity compared to dry air of 50% humidity. The connection of this microscopic process with the electronic degradation of the material during solar cell processing will be discussed.

Keywords: Chalcopyrites; $CuGaSe_2$; Electron-paramagnetic resonance; Extrinsic and intrinsic defects; Solar cells

1. Introduction

The compound semiconductor $CuGaSe_2$ crystallises in the chalcopyrite structure and exhibits optoelectronic properties that qualify the material to be used as thin-film solar-cell absorbers. The band gap energy of 1.68 eV or 738 nm at room temperature lies at the NIR edge of the visible spectrum, the absorption coefficient is larger than 10^4 cm^{-1} for $\lambda < 740$ nm and values up to 80 cm^2/V s have been achieved for charge carrier mobilities of synthetic single crystals [1]. Solely p-type $CuGaSe_2$ thin films and crystals have been produced and attempts for n-type doping failed so far [2]. Laboratory-scale thin-film solar cells making use of $CuGaSe_2$ absorbers reached energy conversion efficiencies of 9.3 % [3]. An improvement in the understanding of the material's defect physics and recombination kinetics is considered to be a key issue for further progress in solar cell efficiencies. For this purpose electron-paramagnetic resonance (FPR) and light-induced EPR (LEPR) investigations were started with $CuGaSe_2$ bulk material. EPR has already been successfully applied to study intrinsic and extrinsic defects in sulphur-containing chalcopyrite compounds [4–10]. With respect to solar-cell applications EPR investigations on $CuInSe_2$ were carried out [11–15]. Only recently, the first EPR study on $CuGaSe_2$ was performed [16] that led to the identification of two transition metal ion contamination Ni^+ and Fe^{2+} and their associated EPR parameters. Moreover, a pronounced ageing effect was observed for $CuGaSe_2$ powders, which may be of relevance for solar-cell applications of the material. In this work, the ageing effect of the material will be presented in more detail and the first light-induced EPR investigations on Ni^+:$CuGaSe_2$ will be demonstrated.

2. Experiments and discussion

The results presented in this work have been obtained with intentionally undoped material that was synthesised from highly pure elements (6*N* Cu, 7*N* Ga, 5*N* Se) without addition of chemical transport agents by virtue of a two-step process at 1100 and 900°C, for further details see [17]. Material was stringently processed either in the inert atmosphere of a glove box or under high vacuum conditions. It was attempted by this procedure to avoid any contact of the sample with ambient air which has been reported to cause a degradation of $CuGaSe_2$ solar-cell absorbers [3]. As-grown lumps and powder material of defined grain size (<80 μm) have both been measured by EPR, the latter of which had been obtained by mortaring and sieving the first. Both sorts

* Corresponding author. Tel.: + 49-30-6705-3309; fax: + 49-30-6705-3333.

E-mail address: birkholz@hmi.de (M. Birkholz)

0040-6090/00/$ - see front matter
PII: S0040-6090(99)00781-6

of samples were inserted into Suprasil quartz glass ampoules which were evacuated to high vacuum and sealed. EPR spectra were taken with a Bruker Elexys 500 system operating at X-band microwave frequencies. For measurements of large-crystalline $CuGaSe_2$ lumps the spectrometer was equipped with a goniometer head to vary the orientation of internal symmetry axes within the material with respect to the applied external magnetic field H_0.

The EPR spectrum of a $CuGaSe_2$ powder sample measured at a temperature of 5 K is given at the top of Fig. 1. In the spectrum three distinct signals can be distinguished. Besides the Ni^+ centre identified in [16] two isotropic signals are present which have been named by letters C and D. Their microscopic nature is currently under investigation. We will not consider both signals in the following except for making use of the perfect Lorentzian line shape of the isotropic C signal having its centre at $g = 2.034$ and a line width of some hundred G. The C signal has been subtracted from the spectrum as presented in Fig. 1, where the Ni^+ signal can now be fully recognised. It has an axially symmetric g-tensor with $g_{xx} = g_{yy} = g_\perp > g_\parallel = g_{zz}$. The principal components $g_\perp$ and $g_\parallel$ of the g-tensor are determined by the low field and the high field peak of the powder pattern to amount to $g_\perp = 2.3478(5)$ and $g_\parallel = 1.869(1)$, respectively. The Ni^+ signal amplitude was found to decrease with increasing temperature stronger than $1/T$ due to a line broadening effect and was undetectable for $T > 40$ K. This served as an additional proof for the correct extraction of the Ni^+ powder pattern from the measured total spectrum. For reasons of clarity the high-field part of the spectrum is enlarged in the figure. At the bottom of Fig. 1 a simulated spectrum is shown that has been calculated with the g-tensor components mentioned above and line width ΔH_{pp} of 38 and 76 G for $g_\perp$ and $g_\parallel$, respectively. The agreement between the measured and simulated spectrum is seen to be excellent. As has been shown, [16] we assign this signal to a Ni^+ contamination of our samples with Ni^+ ions residing on metal lattice sites. EPR transitions at $g_\perp$ occur for grains with their crystallographic c-axis parallel to the magnetic field, while the transitions at $g_\perp$ are due to grains with H_0 lying within the ab plane. The spin density of the paramagnetic impurities was deduced from the spectrum to amount to approximately 0.5 ppm or $2 \times 10^{16} cm^{-3}$, which was found to compare with the Ni concentration independently measured by inductively-coupled plasma mass-spectroscopy (ICP-MS).

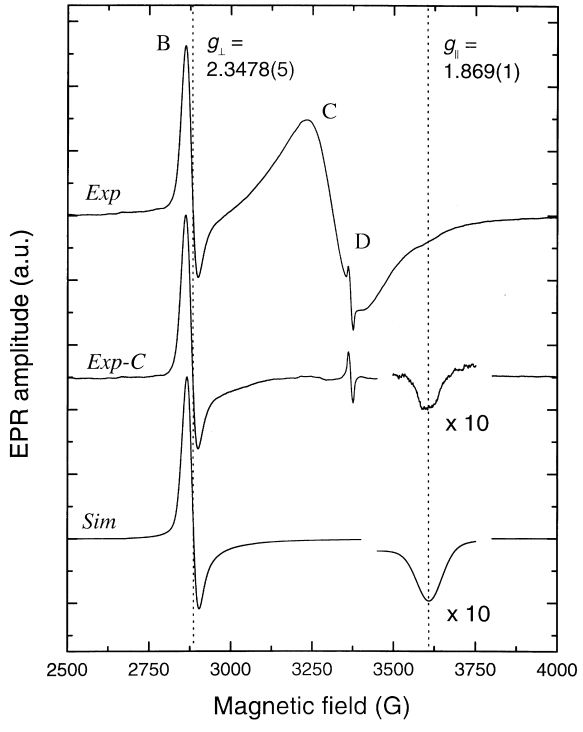

Fig. 1. EPR spectra of $CuGaSe_2$ powder at 5 K. The top spectrum is the measured one, while the middle spectrum has been obtained from experiment by subtracting the C signal. The bottom spectrum gives the simulation of a $S = 1/2$ centre with g-tensor components as indicated.

The earlier EPR work on Ni in chalcopyrite compounds as $CuGaS_2$ and other sulphides made use of an intentional Ni doping [8,18,19]. In contrast to this procedure the nickel contamination in our $CuGaSe_2$ samples was unintended and most probably introduced with the contamination of one of the source elements. We expect that Ni^+ impurities could be detected within $CuGaSe_2$ powders by EPR down to concentrations of about 10^{14} cm^{-3}. It will depend upon further investigations with respect to the recombination properties of Ni^+ centres whether such a high-sensitivity control tool like EPR is necessary for the successful preparation of $CuGaSe_2$ devices.

In order to investigate the significance of Ni^+ centres for the electronic properties of $CuGaSe_2$ light-induced EPR measurements (LEPR) were performed. Experiments were carried out on a lump of approximately 1.5 mm diameter which was oriented in the cavity such that a minimum resonance field was obtained causing a maximum signal amplitude and a minimum line width. The sample was illuminated by a 680 nm laser diode with a maximum photon flux of 5×10^{17} cm^{-2} s^{-1}. Although the penetration depth at this wavelength is on the order of μm, the Ni^+ signal was quenched to 64% at maximum photogeneration rate (see Fig. 2a). No additional resonance was observed in the LEPR spectra. Therefore, we exclude that the quenching accounts for a charging of Ni^+ to Ni^{2+} ($3d^8$, $S = 1$), which is also paramagnetic and should occur in the spectrum. Ni^0 with a $3d^{10}$ electronic configuration and $S = 0$, however, is not paramagnetic and we conclude that the observed quenching is due to a charging from Ni^+ to Ni^0. It appears unlikely that the observed Ni^+ spin density and the light-induced quenching of the signal would solely result from the illuminated outer shell of the lump. On the contrary, the nickel ions must be assumed to be homogeneously distributed within the sample due to the high-temperature growth of material. From these considerations we conclude that the large quenching is caused by excess carriers diffusing into a considerable – unilluminated – fraction of the sample

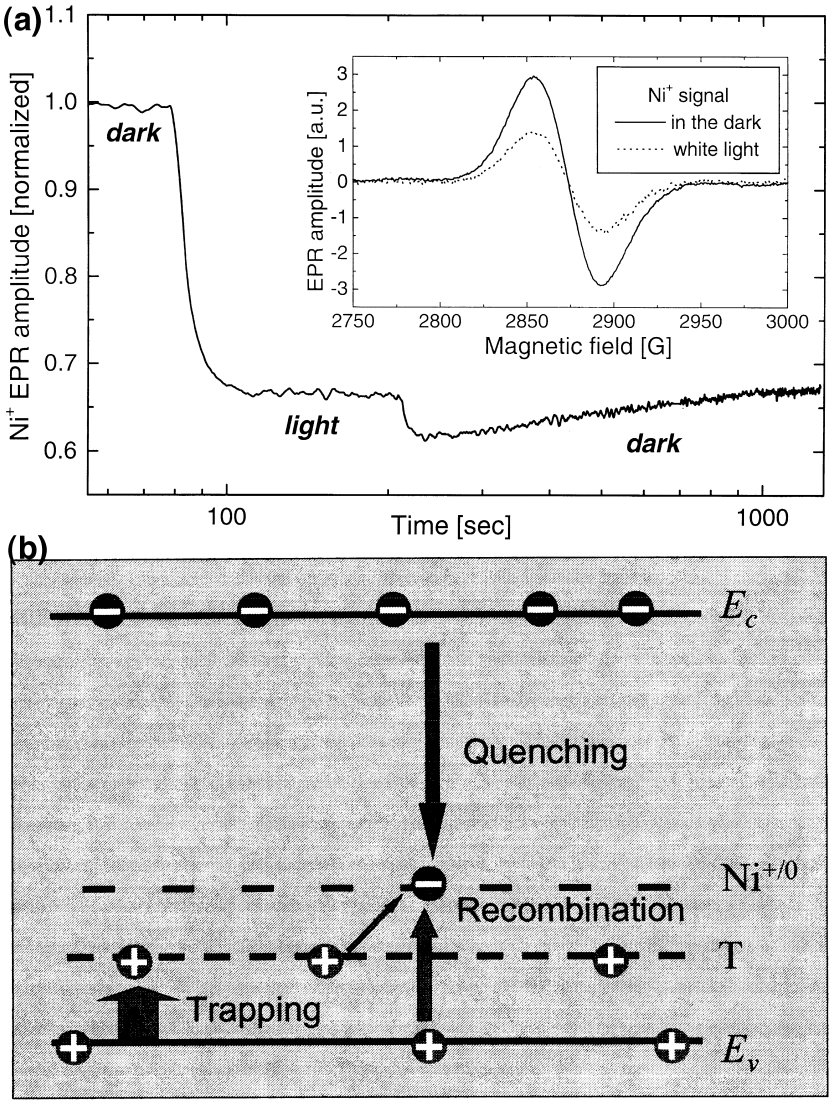

Fig. 2. (a) Transient of Ni^+ EPR signal amplitude in the dark under illumination and in the dark again. The inset displays the steady-state spectra in the dark and under illumination of a $CuGaSe_2$ crystallite. (b) Energy gap model for Ni^+/Ni^0 level and hole trap in $CuGaSe_2$, for a discussion see text.

volume. This would require their diffusion length to be of the same order of magnitude than the sample diameter.

Varying the photon flux over three orders of magnitude resulted in a change of the quenching (A_{light}/A_{dark}) from 92 to 64%. If the Ni^+ centre would be a shallow electron trap not involved in recombination, one would expect a complete quenching at a temperature of 5 K where re-emission into the band should be negligible. The observation that the quenching amplitude only weakly depends on the generation rate is most easily explained by assuming Ni^+ to act as a recombination centre: (i) relaxation of an electron from the conduction band edge into the Ni^+ level leads to quenching of the EPR signal while (ii) recombination with a hole transforms the unobserved Ni^0 to Ni^+ again. Because an increase of light intensity generates as many surplus electrons as holes, both processes are accelerated and the net occupation of the Ni level should only change in a minor way. In Fig. 2a we present a transient of the Ni^+ peak under varying illumination conditions, which was obtained by setting the magnetic field to a constant value and monitoring the EPR amplitude as a function of time. After t_1 the photogeneration is turned on and the signal is quenched as described above. Surprisingly, after tuning off the light at t_2 again the signal does not increase immediately, but is further quenched to 59%. In the following the signal starts to recover, but this process occurs on a time scale of hours. Thus, immediately after stopping the photogeneration the electron trapping process is still efficient while the recombination step seems to be hindered.

All experimental observations may be explained within a simple model if we assume an additional hole trap to act between the valence band edge and the $Ni^{+/0}$ level. The second quenching after switching off the light may be understood in terms of this model by a competition between

the trap and Ni^0 for the capture of free holes which concentration starts to decrease after t_2. If the product of density and cross section for hole capture $N\sigma_h$ of the traps is assumed to be larger than the same quantity of Ni^0, the second quenching can be understood. The second effect to account for is the conversion of Ni^0 to Ni^+ after the additional quenching that takes place on a very slow time scale. In our model this process would be associated either with a reemission from the trap into a mobile valence band state or a direct transition of a hole from the trap to Ni^0. The former can be regarded as being nearly absent at $T = 5$ K and the latter may be of very low probability, too, for instance due to a large geometrical spacing. Summarising we can account for our observations within the model given in Fig. 2b involving excess carriers in the conduction and valence band, a $Ni^{+/0}$ level which acts as a recombination centre and an efficient hole trap. Note that the position of the $Ni^{+/0}$ level within the forbidden gap cannot be determined from our measurements yet. Our model just restricts the level to be located between the conduction band edge and the additional hole trap level.

The cupric ion Cu^{2+} was identified as another EPR active centre in $CuGaSe_2$, although its occurrence could only be detected within powders exposed to ambient air [16]. It has been supposed that this ageing behaviour may be correlated with the degradation of $CuGaSe_2$ solar cells which occurs when the thin absorber film is exposed to air prior to the emitter deposition. In order to investigate this ageing process two powder samples were stored at room temperature in desiccators with different humidity and EPR spectra of both samples were taken after different times. Both samples originated from the same synthesis and have been stored under high-vacuum conditions prior to the experiment. In case of sample A the bottom of the desiccator was covered with tridestilled H_2O causing a humidity of almost 100% to which the powder was exposed. In the case of sample B the humidity within the desiccator was reduced to values of about 50%. After 1, 2, 4 and 16 days EPR spectra were measured.

EPR spectra of sample A and B after 16 days are shown in Fig. 3a together with a spectrum of the virgin sample prior to air exposition. The change in the spectrum of sample A with time is dominated by an apparent shift of the C signal towards smaller fields or larger g values. In addition, the $g_\perp(Ni^+)$ signal seems -to vanish which will not be considered here any further. The shift of the spectrum has almost saturated after 2 days in case of sample A. We interpret the shift of the C signal by assuming a new signal to develop with increasing time at higher g-values causing the signal to become a superposition of the former C signal and the new signal accounting for a set of paramagnetic centres introduced by ageing. In Fig. 3b the structure of the newly introduced signal is presented that has been obtained by subtracting the C and D signals from the 16-day spectrum of sample A. The paramagnetic centre introduced by ageing of $CuGaSe_2$ powder displays the typical features of a Cu^{2+} powder spectrum, compare [20–22]. Both naturally occurring isotopes ^{63}Cu and ^{65}Cu have a nuclear spin of $I = 3/2$ which should cause a hyperfine splitting of the ^2D electronic state into groups of four lines. However, due to large line widths of transition metal ions in chalcopyrite compounds and due to the isotropic averaging of all orientations, the hyperfine splitting cannot be resolved, but instead the some hundred G broad signal is observed. The simulation of the spectrum with a rhombic g-tensor, $g_{xx} = 2.07(1)$, $g_{yy} = 2.18(2)$, $g_{zz} = 2.40(5)$, and hyperfine coupling constants $A_{xx} = A_{yy} \approx 30$ and $A_{zz} = 140(5)$ G is also shown in the Fig. 3b. The agreement with the measured spectrum is satisfying. The observed spectral shift was considerably slower for sample B (see Fig. 3a), the 16-day spectrum of which

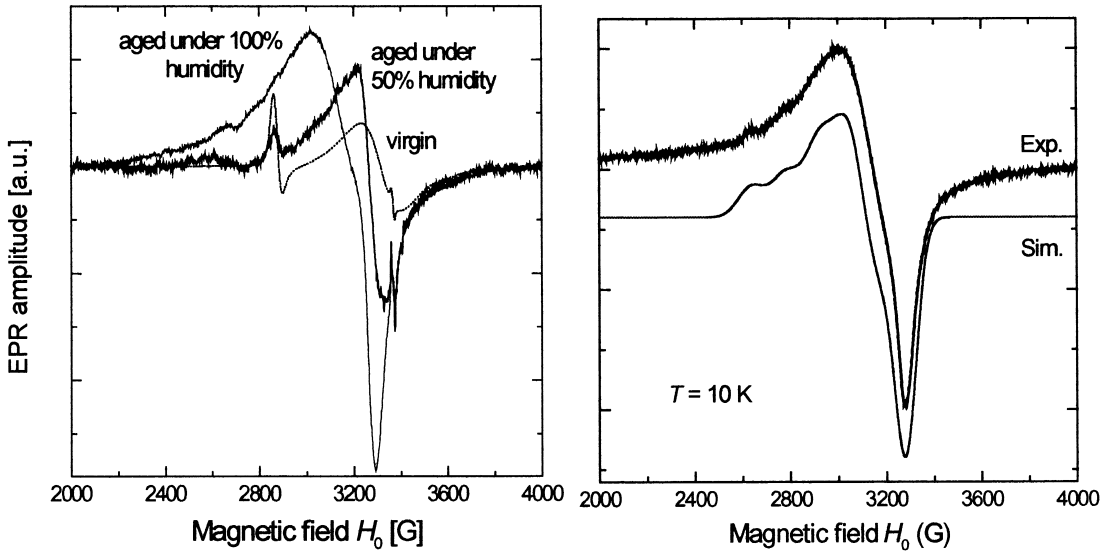

Fig. 3. (a) EPR spectra of aged $CuGaSe_2$ samples A and B and a sample unexposed to air. (b) Difference spectrum of aged and virgin sample together with a simulation of a Cu^{2+} powder signal exhibiting line parameters given in the text.

resembled to the 1 day spectrum of sample A. We conclude that a subset of formerly all Cu^+ ions contained in the sample has been oxidised to Cu^{2+} by contact with wet air and that humidity appears as the main cause of the process.

Regarding the microscopic interpretation of the spectra of aged $CuGaSe_2$ samples two aspects are of relevance. Firstly, the effect of ageing has so far only be observed in EPR spectra of powders having a larger ratio of surface to volume than as-grown lumps. Secondly, no satisfying agreement between measured and simulated spectra could be obtained by assuming an axial symmetric g-tensor ($g_{xx} = g_{yy} = g_{zz}$) as it would be appropriate for the tetragonal co-ordination, D_{2d}, of copper atoms in the undisturbed chalcopyrite structure. However, a rhombic g-tensor, $g_{xx} \neq g_{yy} \neq g_{zz}$, has to be introduced indicating that the valence change from $+1$ to $+2$ is accompanied by a change in local bonding symmetry. Both observations imply that the ageing of $CuGaSe_2$ powders is associated with the oxidation of surface copper atoms.

The precise microscopic reaction mechanism and the end product of the oxidation process cannot be concluded from EPR powder spectra. The complex chemistry of Cu^{2+} knows a large variety of oxocomplexes and aquo-complexes which derive from a distorted tetrahedral co-ordination [23,24]. H_2O molecules that have been identified to accelerate the ageing process may play the role of finally bonded ligands or they may act as catalyst for the bonding of oxygen ions to the central Cu^{2+}. To clarify these questions, more surface sensitive methods have to be applied to develop a microscopic picture of the surface oxidation. Regarding the kinetic of the reaction it may be deduced from the sequences of spectra that the main oxidation step for sample A has already occurred after one day. The time constants for the surface oxidation of $CuGaSe_2$ powders having grain sizes in the range of μm would accordingly lie in the order of hours than in the order of days. This is the same time scale as it was identified for the degradation of V_{oc} and I_{sc} of $CuGaSe_2$ solar cells, if the absorber layer was exposed to air for different times prior to the deposition of the CdS absorber layer [3]. This comparison implies that the ageing mechanism of $CuGaSe_2$ absorbers is associated with the oxidation of Cu ions as observed by the EPR measurements presented above.

3. Conclusion

In conclusion, we have presented LEPR investigation of the Ni^+ centre and EPR investigations of the Cu^{2+} centre in $CuGaSe_2$. The experimental observations indicate the nickel ion to act as recombination centre for photogenerated charge carriers. Powder surfaces of $CuGaSe_2$ exposed to air exhibited a pronounced oxidation of copper ions. The ageing was strongly accelerated in air of 100% humidity. The time scale of the oxidation compares with the time scale of degradation of uncoated $CuGaSe_2$ solar-cell absorbers.

References

[1] J.H. Schön, E.P. Baumgartner, E. Arushanov, H. Riazi-Nejad, C. Kloc, E. Bucher, Cryst. Res. Technol. 31 (1996) 155.
[2] J.H. Schön, F.P. Baumgartner, E. Arushanov, H. Riazi-Nejad, C. Kloc, E. Bucher, J. Appl. Phys. 79 (1996) 6961.
[3] V. Nadenau, D. Hariskos, H.W. Schock, in: H. Ossenbrink, P. Helm, H. Ehmann (Eds.), 14th EC Photovoltaic Solar Energy Conf., Barcelona, Stephens & Associates, Bedford, UK, 1997.
[4] J. Schneider, A. Räuber, G. Brandt, J. Phys. Chem. Sol. 34 (1973) 443.
[5] G. Brandt, A. Räuber, J. Schneider, Solid State Comm. 12 (1973) 481.
[6] U. Kaufmann, A. Räuber, J. Schneider, Solid State Comm. 15 (1974) 1881.
[7] H.J. von Bardeleben, A. Goltzene, C. Schwab, J. Physique (Coll.) 36 (1975) C3.
[8] U. Kaufmann, Phys. Rev. B11 (1975) 2478.
[9] H.J. von Bardeleben, A. Goltzene, C. Schwab, Phys. Status Solidi 76 (1976) 363.
[10] G.L. Troeger, R.N. Rogers, H.M. Kasper, J. Phys. C: Solid State Phys. 9 (1976) L73.
[11] H.J. von Bardeleben, R.D. Tomlinson, J. Phys. C: Solid State Phys. 13 (1980) L1097.
[12] J.M. Tchapkui-Niat, A. Goltzene, C. Schwab, J. Phys. C: Solid State Phys. 15 (1982) 4671.
[13] G.K. Padam, G.L. Malhotra, S.K. Gupta, Sol. Energy Mater. 22 (1991) 303.
[14] Y.J. Hsu, H.L. Hwang, J. Appl. Phys. 66 (1989) 5798.
[15] N. Nishikawa, I. Aksenov, T. Shinzato, T. Sakamoto, K. Sato, Jpn. J. Appl. Phys. 34 (1995) L975.
[16] M. Birkholz, P. Kanschat, T. Weiss, M. Czerwensky, K. Lips, Phys. Rev. B59 (1999) 12268.
[17] T. Weiss, M. Birkholz, M. Saad, et al., J. Cryst. Growth 198/199 (1999) 1190.
[18] H.J. von Bardeleben, C. Schwab, A. Goltzene, Phys. Lett. 51 A (1975) 460.
[19] G.L. Troeger, R.N. Rogers, H.M. Kasper, J. Phys. C: Solid State Phys. 8 (1975) L222.
[20] I.H. Parker, J. Phys. C: Solid State Phys. 4 (1971) 2967.
[21] F.J. Owens, J. Appl. Phys. 53 (1982) 368.
[22] S.K. Hoffmann, J. Goslar, L.S. Szczepaniak, Phys. Rev. B37 (1988) 7331.
[23] F.A. Cotton, G. Wilkinson, Advanced Inorganic Chemistry, Wiley, New York, 1972.
[24] M. Becke-Goehring, H. Hoffmann, Komplexchemie, Springer-Verlag, Berlin, 1970.